Effects of Molecular Weight of Polysulfone on Phase Separation Behavior for Cyanate Ester/Polysulfone Blends

J. W. HWANG,[1] K. CHO,[1] T. H. YOON,[2] C. E. PARK[1]

[1] Polymer Research Institute, Department of Chemical Engineering, Electrical and Computer Engineering Division, Pohang University of Science and Technology, San 31, Hyoja-Dong, Pohang 790-784, Korea

[2] Department of Materials Science and Engineering, Kwangju Institute of Science and Technology, 1 Oryong-dong, Puk-gu, Kwangju 500-712, Korea

Received 3 August 1999; accepted 19 November 1999

ABSTRACT: The effects of molecular weight of polysulfone (PSF) on the morphology of bisphenol-A dicyanate (BADCy)/PSF blends were studied. Because the viscosity of the blend increased and the miscibility between BADCy and PSF decreased with the increase of PSF molecular weight, these two competing effects on the phase-separation were investigated. It was observed that the effect of viscosity was predominant: the viscosity of the blends at the onset point of phase separation increased with the increase of PSF molecular weight. The phase separation mechanism depends on the viscosity of the blends at the onset point of phase separation and determines the morphology of the blends. Because the increasing viscosity with increasing the molecular weight of PSF suppressed the nucleation and growth even with 10 phr of PSF content, phase separation occurred through spinodal decomposition to form the combined morphology having both PSF particle structure and BADCy particle structure. The combined morphology and the BADCy particle structure were obtained with a smaller amount of high molecular weight PSF content. This indicates that the viscosity of the blends at the onset point of phase separation is the critical parameter that determines the morphology of the blends. © 2000 John Wiley & Sons, Inc. J Appl Polym Sci 77: 921–927, 2000

Key words: phase separation; cyanate ester; polysulfone; viscosity

INTRODUCTION

Cyanate ester resins are currently used for many important application such as adhesives, encapsulants of electronic devices, high-temperature adhesives, and advanced composite matrices in aerospace industry. The cyanate ester monomers undergo polycyclotrimerization to form highly crosslinked polycyanurates.[1–3] Highly crosslinked networks of cyanate esters possess excellent thermal and chemical stability as well as high strength and modulus.[1–8] However, their widespread use is unfortunately limited in many applications by their inherent brittle behavior.

To toughen the highly crosslinked thermosets such as cyanate esters, bismaleimides, and multifunctional epoxy resins, many researchers have employed the rubber toughening without success because the yielding of thermoset matrices cannot be induced owing to their highly crosslinked structures.[9–12] Besides, the use of rubber as toughening agent results in drastic reduction in glass transition temperature and mechanical strength. Therefore, toughening of highly crosslinked thermosets was explored by physical

Correspondence to: C. E. Park.

Contract grant sponsors: The Ministry of Education Research Funds for Advanced Materials; BK 21 program.

Journal of Applied Polymer Science, Vol. 77, 921–927 (2000)

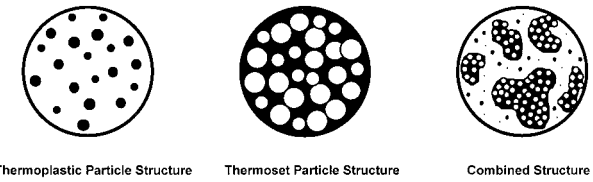

Figure 1 Schematic diagrams of morphologies of thermoset/thermoplastic blends.

blending with thermoplastics such as poly(ether imide),[13–15] poly(arylene ether ketone),[16] poly(ether sulfone),[17–20], and polysulfone (PSF).[20] The improvement in fracture toughness by making polymer alloys of thermosets with thermoplastics is achieved without the expense of modulus. Generally, the thermoset and thermoplastic blends are homogeneous at the beginning of curing. In the curing process of thermoset resins, the increasing molecular weight of the thermoset component initiates the phase separation to generate various heterogeneous two-phase morphologies. Then these morphologies, developed by the reaction-induced phase separation, would be fixed at a certain stage of curing by gelation and vitrification of thermoset resins.

The fracture toughness of cured thermoset/thermoplastic blends is determined by the morphology formed by the consequence of phase separation, which takes place either by nucleation and growth (NG) or the spinodal decomposition (SD) mechanism. The morphology of thermoset/thermoplastic blends depends on composition, curing temperature, pressure, and molecular weight of thermoplastics. Figure 1 shows the three types of schematic morphologies found in thermoset/thermoplastic blends. Generally, the thermoplastic-particle structure is obtained via NG at low content of thermoplastic and the thermoset-particle structure is obtained via SD at high content of thermoplastic. The combined structure having both the thermoplastic-particle structure and the thermoset-particle structure is obtained with intermediate content of thermoplastic.[20–22] The thermoset-particle structure shows the highest fracture toughness and the combined structure shows the next.[13]

The various elements that influence the thermodynamics and kinetics of phase separation during curing of thermosets need to be understood to achieve an optimum heterogeneous structure. Phase separation is induced by increasing the molecular weight of thermosets during curing, i.e., the miscibility of thermoset/thermoplastic blends is altered continuously since the phase diagram moves downward or upward depending on the chemical structures of the blends with the progress of thermoset curing. Therefore, in order to control the morphology of the blends, the alternation of phase diagram and the phase separation mechanism should be studied. In our previous results,[23] the decrease of curing temperature increased the viscosity of blends at the onset point of phase separation, and then the increased viscosity suppressed the nucleation and growth of the blends at the initial stage of phase separation. Therefore, even if the blends had the low content of thermoplastic, the blends were phase separated by SD and formed the thermoset-particle structure or the combined morphology when the blends were cured at low temperature.

In this study, the effects of the molecular weight of PSF on the morphology and the phase-separation behavior of bisphenol-A dicyanate (BADCy)/PSF blends are investigated.

EXPERIMENTAL

Materials

The BADCy monomer with a purity of 99.9% as a crystalline powder was supplied by Ciba-Geigy under the trade name of AroCy B-10. Two kinds of commercial polysulfone (Udel P-1700 and Udel P-3500) were purchased from Rhone Poulenc. Figure 2 shows the chemical structures of BADCy and PSF. Polysulfones were synthesized from bisphenol-A and 4,4′-dichlorodiphenyl sulfone. High purity bisphenol-A was obtained from either Union Carbide Corporation or Dow Chemical

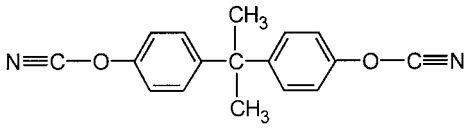

Bisphenol-A dicyanate (BADCy)

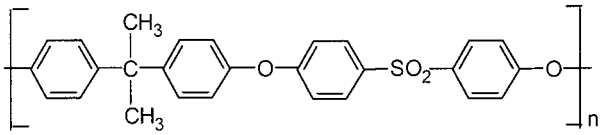

Polysulfone (PSF)

Figure 2 Chemical structure of BADCy and PSF.

Table I Characteristics of the PSF Samples

PSF	Synthesis I	Udel P-1700	Udel P-3500	Synthesis II
M_n[a]	8,500	14,200	16,200	61,500
M_w[a]	38,900	55,500	66,100	84,400
Polydispersity[a]	4.54	3.91	4.07	1.37
$[\eta]_{CHCl_3,\ 25°C}$	0.366	0.475	0.529	0.616
T_g (°C)$_{\text{by DSC}}$	184.1	185.3	186.8	190.5
Nomenclature	PSF39K	PSF56K	PSF66K	PSF84K

[a] M_n, M_w, and polydispersity measured by GPC using polystyrene standard.

Company and recrystallized from toluene. The4,4′-dichlorodiphenyl sulfone was kindly supplied by Amoco Corporation and was recrystallized from toluene.

Synthesis of Polysulfones

A typical synthesis of a chloroterminated polysulfone was conducted in a four-neck, 500 mL, round-bottom flask equipped with a mechanical stirrer, nitrogen inlet, thermometer, Dean Stark trap, and condenser.[24] The flask was charged with bisphenol-A and excess 4,4′-dichlorodiphenylsulfone. The exact amount of each monomer was calculated to control the molecular weight of polymer. 1-Methyl-2-pyrrolidinone was used as a solvent after distillation over calciumhydride, and toluene was used as an azeotroping agent. Finally, 15% excess of potassium carbonate (K_2CO_3) was added as a catalyst. The temperature of the reaction was raised until the toluene began to reflux, which was approximately 130–140°C. Refluxing was continued until no more water was removed from the reaction mixture, which took approximately 4 h at these temperatures. And then, the reaction mixture reacted at 170°C for 12 h. A light brown polymer solution was diluted with chloroform and filtered to remove salts. Prior to precipitation into methanol/water mixture, polymer solution was neutralized by adding a few drops of glacial acetic acid. Upon filtering, the polymer powder was dried at room temperature for over night and in vacuum oven at 175°C for 12 h.

To obtain the higher molecular weight of PSF than Udel P-3500, the precipitation method was used. At first, the synthesized PSF was dissolved in methylene chloride, and then n-hexane as a nonsolvent was slowly added with vigorous stirring until the powder of precipitation settled down to the bottom. After filtering, the precipitation was dissolved again in methylene chloride and then reprecipitated in n-hexane. The precipitation was then dried for 12 h in a vacuum oven at 120°C.

Molecular weights of commercial and synthesized PSFs were measured by gas permeation chromatography (GPC) in tetrahydrofuran solvent using polystyrene standards. And the inherent viscosity of PSFs was measured at 25°C in chloroform as a solvent using Ubbelohode viscometer. The four different molecular weights of PSF are listed in Table I.

Sample Preparation of BADCy/PSF Blends

PSF was dissolved in methylene chloride and mixed with BADCy at room temperature. The solution was heated in an oil bath for 1 h at 120–130°C to drive off most of the methylene chloride, and then the residual solvent and the air bubble were removed under vacuum for 30 min above 130°C. The blended resins were poured in a Teflon-coated aluminum plate and then were cooled down to room temperature.

Conversion Measurement of BADCy Resins

The Fourier transform infrared (FTIR) studies were performed using a Bio-Rad FTS375C spectrophotometer with KBr pellets containing the finely ground material.[24] The C—H stretching band at 2970 cm^{-1} was used as an internal standard. Infrared absorption of nitriles (—CN stretching vibration) appears as double bands at 2270 and 2236 cm^{-1}. Conversions were calculated using the height of 2270 cm^{-1} band with respect to the height of the reference band of 2970 cm^{-1}. If the peak height is directly proportional to the concentration, the conversion of dicyanate func-

tional group at different times can be calculated as

$$P = 1 - \frac{A(t)_{2270}/A(0)_{2270}}{A(t)_{2970}/A(0)_{2970}}$$

where $A(t)_{2270}$ is the absorbance intensity at 2270 cm^{-1}at time t, $A(t)_{2970}$ is the absorbance intensity at 2970 cm^{-1} at time t, $A(0)$ is the initial absorbance intensity, and P is the extent of conversion of dicyanate functional groups.

Morphology

The morphology of BADCy/PSF blends was observed at 200°C isothermal curing by scanning electron microscope (SEM, Hitachi S-2460N). The PSF content was varied as 10, 15, 20, and 30 parts per hundred resins (phr).

Viscosity at the Onset Point of Phase Separation

Cloud point in the light scattering experiment was used as the onset point of phase separation. At the cloud point of BADCy/PSF blends cured isothermally at 200°C, the partially cured blends was taken out from the heating stage of light scattering apparatus and quenched into water at room temperature. Then, the viscosity of partially cured BADCy/PSF blends at the cloud point was measured at the curing temperature of 200°C by a Rheometrics Dynamic Spectrometer (RDS II) using 25 mm circular disks in an oscillating parallel-plate with the rate of 10 radians/s.

RESULTS AND DISCUSSION

In our previous work,[23] the effects of the PSF content and curing temperature on the morphology of BADCy/PSF blends were investigated. It was shown that the viscosity of BADCy/PSF blends at the onset point of phase separation determined the morphology of BADCy/PSF blends. When the viscosity of BADCy/PSF blends was low at the onset point of phase separation, the blends were phase separated by NG to form the PSF-particle structure. When the viscosity of blends was relatively high, the blends were phase separated by SD to form the BADCy-particle structure. With the intermediate viscosity, the combined morphology having both PSF particle structure and BADCy particle structure was formed by two-step processes of phase separation.

In this study, the effects of molecular weight of PSF on the morphology of BADCy/PSF blends are studied. The increase of the molecular weight of PSF increases the viscosity of BADCy/PSF blends, which suppresses the phase separation of the blends. However, the increase of the molecular weight of PSF reduces the miscibility between BADCy and PSF, which accelerates the phase separation of the blends. Therefore, the two competing effects on the morphology of the blends are investigated.

It can be observed in Table I that the two kinds of commercial PSFs and the two kinds of self-synthesized PSFs have different molecular weight to each other. All PSFs have the same repeating units and each PSF is named according to its weight-average molecular weight.

Phase Diagram

Homogenous BADCy/PSF blends having different content of PSF and molecular weight of PSF were prepared. And then, each sample was isothermally cured at 200°C in the hot stage of the light scattering apparatus, and the homogeneous blend is taken out just before the cloud point and quenched into the water of room temperature. To obtain the conversion of BADCy at the onset point of phase separation, the nitrile absorption (2270 cm^{-1}) at the cloud point was measured by FTIR. The viscosity of the blends at the cloud point was measured by RDS at 200°C. The phase diagram of BADCy/PSF blends at 200°C isothermal curing is shown in Figure 3. As the molecular weight of PSF increases, the phase-separation curve moves downward. It indicates that the drop of miscibility between BADCy and PSF, by increasing the molecular weight of PSF, decreases the BADCy conversion at the onset point of phase separation. The decrease of conversion is more pronounced with 10 phr of PSF content than with higher PSF content. With more than 20 phr of PSF content, the effect of miscibility drop is buried due to the high viscosity of the blends.

Figure 3 shows that the critical content of PSF indicating the minimum of each phase curve decreases with the increase of PSF molecular weight. The critical content of PSF is 15 phr of PSF content with BADCy/PSF66K blends and less than 10 phr of PSF content with BADCy/PSF84K blends.

Morphology of BADCy/PSF Blends

The morphology of the cured BADCy/PSF blends was observed with a scanning electron micro-

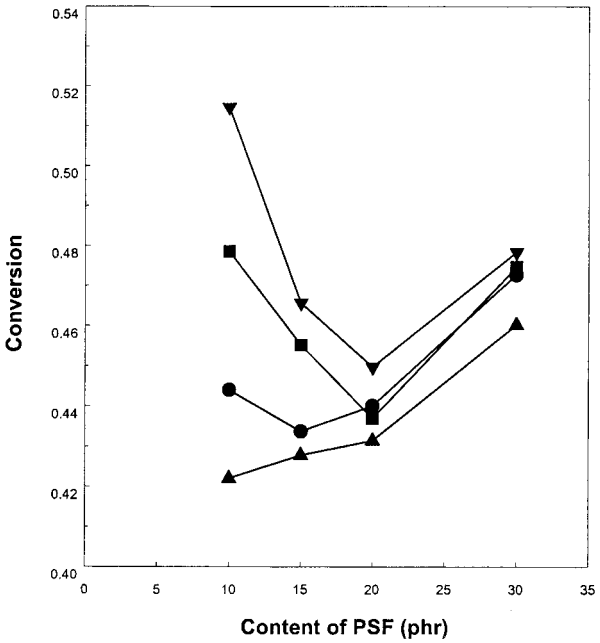

Figure 3 Phase diagram of BADCy/PSF blends at the isothermal curing temperature of 200°C. (▼) BADCy/PSF39K, (■) BADCy/PSF56K, (●) BADCy/PSF66K, and (▲) BADCy/PSF84K.

scope. Figure 4 shows the morphologies of BADCy/PSF blends with various PSF contents and molecular weights of PSF. It has already been reported that the morphology changes from PSF particle structure via combined morphology to BADCy particle structure with the increase of PSF content.[23,34] For the case of the BADCy/PSF56K blend, the morphology is the PSF particle structure with 10 phr of PSF content, and changes to the combined morphology containing both the PSF particle structure and the BADCy particle structure with 15 and 20 phr of PSF content, and the BADCy particle structure with 30 phr of PSF content. The morphology also changes with the increase of the molecular weight of PSF. For the case of BADCy/PSF(15phr) blends, as the molecular weight of PSF increases, the morphology of the blends changes from the PSF particle structure via the combined morphology to the BADCy particle structure. With 10 phr of PSF content, the morphology is the PSF particle structure up to PSF66K and changes to the combined morphology with PSF84K. With 20 phr of PSF content, the morphology is the combined morphology up to PSF56K and changes to the BADCy particle structure from PSF66K.

As the molecular weight of PSF increases, the viscosity of BADCy/PSF blends at the onset point of phase separation increases as shown in Table II. The formation of the PSF particle structure through the nucleation and growth mechanism is suppressed even with 10 phr of PSF84K. Although the phase separation starts in the region of the nucleation and growth, the phase separation is suppressed due to high viscosity. Then, BADCy/PSF84K blend is located in the region of spinodal decomposition in the phase diagram because BADCy polymerizes to have higher molecular weight and the phase diagram moves upward. Therefore, the morphology of the BADCy/PSF84K (10 phr) blend changes from PSF particle structure to the combined morphology. Similarly, as the molecular weight of PSF increases, the combined morphology and the BADCy particle structure are obtained with less amount of PSF content as shown in Figure 4.

From Figure 4 and Table II, the blends having less than 5 Pa · s of viscosity at the onset point of phase separation such as BADCy/PSF39K (10 phr), BADCy/PSF39K (15 phr), BADCy/PSF56K (10 phr), and BADCy/PSF66K (10 phr) blends are phase separated by the nucleation and growth to form the PSF particle structure. The blends having larger than 30 Pa · s at the onset point of phase separation such as BADCy/PSF39K (30 phr), BADCy/PSF56K (30 phr), BADCy/PSF66K (20 phr), BADCy/PSF66K (30 phr), BADCy/PSF84K (15 phr), BADCy/PSF84K (20 phr), and BADCy/PSF84K (30 phr) blends are phase separated by spinodal decomposition to form the BADCy particle structure. The blends having the intermediate viscosity between 10 and 30 Pa · s at the onset of phase separation such as BADCy/PSF39K (20 phr), BADCy/PSF56K (15 phr), BADCy/PSF56K (20 phr), BADCy/PSF66K (15 phr), and BADCy/PSF84K (10 phr) are phase separated by the spinodal decomposition and followed by macro-coalescence, and then have the second phase separation to form the combined morphology. Therefore, the viscosity of BADCy/PSF blends at the onset point of phase separation appears to be a critical parameter to resolve the phase-separation mechanism and the morphology of cured structure, which determines the fracture toughness of the blends.

The effect of molecular weight of PSF on the morphology of the blends was consistent with those of PSF content and temperature showing that the viscosity of the blends at the onset point of phase separation determines the morphology of the blends.

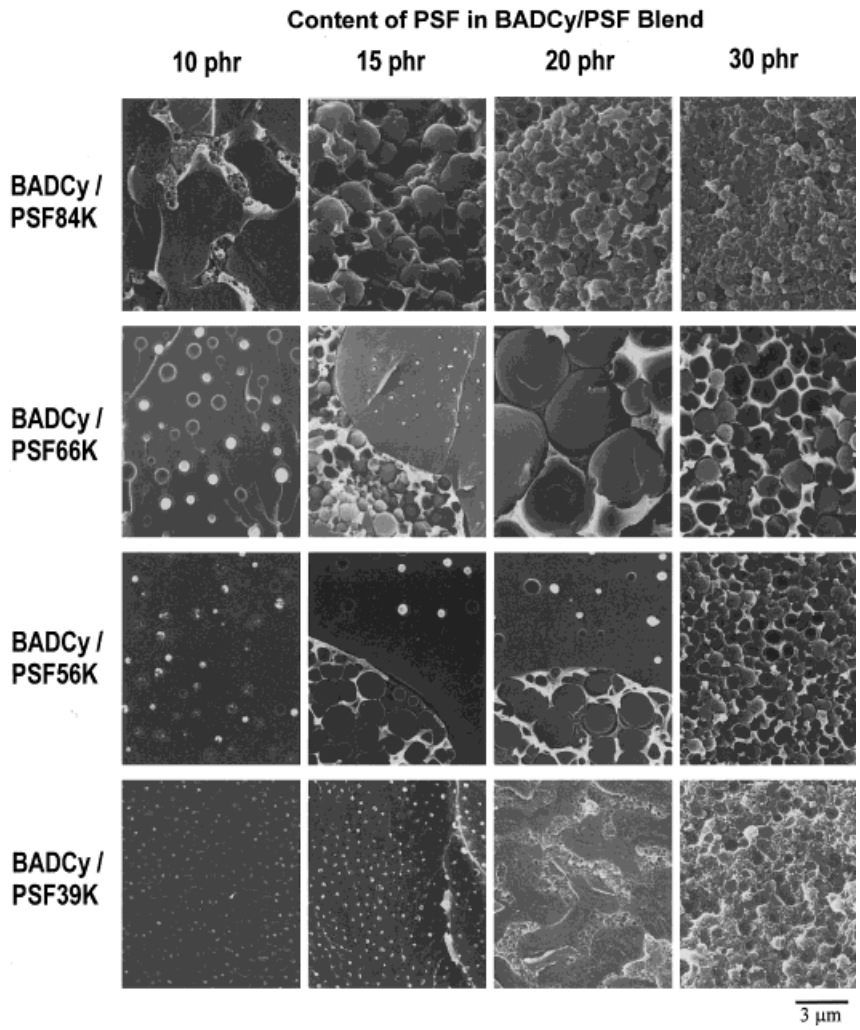

Figure 4 Morphology diagram of BADCy/PSF blends at 200°C isothermal curing.

CONCLUSIONS

Increasing the molecular weight of PSF in the BADCy/PSF blends increased the viscosity of the blends at the onset point of phase separation. Because the viscosity suppressed the nucleation and growth, the PSF particle structure was not formed even with 10 phr of PSF having high molecular weight (PSF84K). Similarly, as the molecular weight of PSF increased, the combined structure and the BADCy particle structure were obtained with a smaller amount of PSF content. The effect of molecular weight of PSF on the morphology of the BADCy/PSF blends was consistent with those of PSF content and temperature showing that viscosity of the blends at the onset point of phase separation determined the morphology of the blends.

Table II Viscosity Values of BADCy/PSFs Blends at Onset Point of Phase Separation at 200°C Isothermal Curing

PSF Content	PSF39K[a]	PSF56K[a]	PSF66K[a]	PSF84K[a]
10 phr	0.335	1.00	3.29	23.7
15 phr	0.891	11.6	19.4	50.1
20 phr	10.2	23.0	32.4	79.9
30 phr	36.2	49.1	89.2	130

[a] Unit: Pa · s.

This work was supported by a research grant from Ministry of Education Research Funds for Advanced Materials, 1998, and partially supported by BK 21 program.

REFERENCES

1. Osei-Owusu, A.; Martin, G. C. Polym Eng Sci 1992, 32, 535.
2. Bauer, M.; Bauer, J.; Jährig, S. Makromol Chem Macromol Symp 1991, 45, 97.
3. Papathomas, K. I.; Wang, D. W. J Appl Polym Sci 1992, 44, 1267.
4. Novak, H. L.; Comer, D. A. Adhesive Age 1990, Feb, 28.
5. McGonnell, V. P. Adv Composites 1992, May/June, 28.
6. Shimp, D. Polym Mater Sci Eng 1994, 71, 623.
7. Graver, R. B. Polym Prepr 1990, 27, 491.
8. Simon, S. L.; Gillham, J. K. J Appl Polym Sci 1993, 47, 461.
9. Pearson, R. A.; Yee, A. F. J Mater Sci 1989, 24, 2571.
10. Kim, D. S.; Cho, K.; An, J. H.; Park, C. E. J Mater Sci Lett 1992, 11, 1197.
11. Kim, D. S.; Cho, K.; An, J. H.; Park, C. E. J Mater Sci 1994, 29, 1854.
12. Kim, D. S.; Cho, K.; Kim, J. K.; Park, C. E. Polym Sci Eng 1996, 36, 755.
13. Cho, J. B.; Hwang, J. W.; Cho, K.; An, J. H.; Park, C. E. Polymer 1993, 34, 4832.
14. Hourston, D. J.; Lane, J. M. Polymer 1992, 33, 1379.
15. Bucknall, C. B.; Gilbert, A. H. Polymer 1989, 30, 213.
16. Srinivasan, S. A.; McGrath, J. E. Polymer 1998, 39, 2415.
17. Yamanaka, K.; Inoue, T. Polymer 1989, 30, 662.
18. Akay, M.; Cracknell, J. G. J Appl Polym Sci 1994, 52, 663.
19. Di Pasquale, G.; Motta, O.; Recca, A.; Carter, J. T.; McGrail, P. T.; Acierno, D. Polymer 1997, 38, 4345.
20. Hwang, J. W.; Park, S. D.; Cho, K.; Kim, J. K.; Park, C. E.; Oh, T. S. Polymer 1997, 38, 1835.
21. Iijima, T.; Miura, S.; Fukuda, W.; Tomoi, M. J Appl Polym Sci 1995, 57, 819.
22. Min, B.-G.; Stachurski, Z. H.; Hodgkin, J. H. J Appl Polym Sci 1993, 50, 1511.
23. Hwang, J. W.; Cho, K.; Park, C. E.; Huh, W. J Appl Polym Sci 1999, 74, 33.
24. Hedrick, J. L.; Yilgor, I.; Jurek, M.; Hedrick, J. C.; Wilkes, G. L.; McGrach, J. E. Polymer 1991, 32, 2020.
25. Chen, Y.-T.; Macosko, C. W. J Appl Polym Sci 1996, 62, 567.
26. Bucknall, C. B.; Gomez, C. M.; Quintard, I. Polymer 1994, 35, 353.
27. Yamanaka, K.; Inoue, T. Polymer 1989, 30, 662.
28. Chen, W.; Kobayashi, S.; Inoue, T.; Ohnaga, T.; Ougizawa, T. Polymer 1994, 35, 4015.
29. Ohnaga, T.; Chen, W.; Inoue, T. Polymer 1994, 35, 3774.
30. Oyanguren, P. A.; Frontini, P. M.; Williams, R. J. J.; Vigier, G.; Pascault, J. P. Polymer 1996, 37, 3087.
31. Elicabe, G. E.; Larrondo, H. A.; Williams, R. J. J. Macromolecules 1997, 30, 6550.
32. Chen, J.-P.; Lee, Y.-D. Polymer 1995, 36, 55.
33. Bennett, G. S.; Farris, R. J.; Thompson, S. A. Polymer 1991, 32, 1633.
34. Hourston, D. J.; Lane, J. M. Polymer 1992, 33, 1379.